This article has been accepted for publication in a future issue of this journal, but has not been fully edited. Content may change prior to final publication. Citation information: DOI 10.1109/LED.2017.2787203, IEEE Electron Device Letters

Adsorption of Small Molecules on Niobium Doped Graphene: A Study Based on Density Functional Theory

Jitendra Kumar, Harshal B. Nemade, *Member, IEEE*, P. K. Giri

***Abstract*—The paper presents the adsorption properties of CO, NH_3, CH_4, SO_2, and H_2S molecules over niobium doped graphene sheet (Nb/G). Using density functional theory, the optimum configuration and orientation of adsorbent molecules over the Nb/G surface are geometrically optimized and adsorption energy, adsorption distance, Hirshfeld charge transfer, electron localization function and the work function of Nb/G-molecule systems are calculated. CO and SO_2 molecules over Nb/G show chemisorption, hence they have high reactivity towards Nb/G. Adsorption of NH_3, CH_4, and H_2S on Nb/G shows physisorption as they are weakly adsorbed. The adsorption of these molecules indicates the suitability of Nb/G as a sensor. To understand the superiority of Nb/G over pristine graphene, comparison of adsorption properties was made between the two systems. The work function of Nb/G with adsorbed molecule suggests that the Fermi level of Nb/G surface may be controlled by the selection of appropriate adsorbent molecules. Therefore, Nb/G could be a good candidate for gas sensing application.**

***Index Terms*—Adsorption, density-functional theory, graphene, niobium doping.**

I. Introduction

Successful synthesis of stable single layer graphene with outstanding mechanical and electronic properties has arisen the interest of research and device community for new applications of this material [1]. Zero band gap two-dimensional material with large surface area for adsorption with modification of conductivity by the absorbent molecules makes it an efficient material for sensing application [2], [3]. Sensing and catalytic properties of graphene is significantly enhanced by embedding transition metal atom to the graphene sheet leading to the graphene based catalyst [4]. A catalyst typically increases the rate of a chemical reaction and catalyzed reactions have a lower activation energy than the corresponding uncatalyzed reaction, resulting in a higher reaction rate. Transition metal is being used as catalyst for several oxidation reduction reaction, fuel cell application and intermediate for spintronic application. Ti and V doped graphene sheets are reported to have increased sensitivity for formaldehyde [5]. Aluminum doped graphene shows high reactivity toward CH_4 molecule [6]. Nb and other transition metal doped graphene surface and Nb atom in graphitic layers are found to be energetically favorable for catalyzing the cathodic oxidation reduction reaction [7], [8]. Two-dimensional $MoSe_2$ layer doped with Nb atoms are found to improve the gas sensing performance [9]. These recent literatures suggest that Nb/G is a promising candidate for graphene based electro-catalytic and gas sensing application. Herein, we investigate the adsorption properties of small adsorbent molecules, viz. CO, NH_3, CH_4, SO_2, and H_2S on the Nb/G surface. Gas sensing is an important process of industrial monitoring for safety of environment and living being nearby. However, to our knowledge no *ab initio* calculation of adsorption properties of these molecules on Nb/G surface has been reported yet.

"We thank MeitY (No. 5(9)/2012-NANO (Vol.II)), Government of India for the financial support."

Jitendra Kumar, is with Center for Nanotechnology, IIT Guwahati, Assam, 781039, INDIA. (e-mail: k.jitendra@iitg.ernet.in).

Harshal B. Nemade, is with Department of Electronics and Electrical Engineering, IIT Guwahati, Assam, 781039, INDIA. (e-mail: harshal@iitg.ernet.in).

P. K. Giri, is with Department of Physics, IIT Guwahati, Assam, 781039, INDIA. (e-mail: giri@iitg.ernet.in).

II. Computational Details

The calculations were carried out with DMol^3 code based on DFT as implemented in material studio [10]. Exchange correlation of generalized gradient approximation (GGA) and PBE functional was employed in our work [11]–[13]. Grimme's dispersion corrected density functional theory (DFT-D) was used for dispersion interaction [14]–[16]. Semi-core pseudo potential treatment with double numeric polarization (DNP) basis set was employed with 4.4 basis file [13], [17]. The optimized and relaxed lattice constant of graphene unit cell used was a=b=2.468 Å, which was in good agreement with experimental value of 2.46 Å [18]. The system contains a 4×4 supercell of graphene doped with a single Nb atom to substitute the carbon atom near the center of supercell, as shown in Fig. 1(a). A vacuum space of 20 Å perpendicular to the graphene plane was placed to minimize the interaction effect between nearby adjacent layers. Spin unrestricted calculation was performed with 9×9×1 Monkhorst-Pack k-point grid sampling in the Brillouin zone for the calculation of electronic properties. Adsorbent molecules were added at a distance of 4 Å above the Nb atom. All the configurations were optimized until the maximum force was less than 0.01 eV/Å. Geometrically relaxed configurations of adsorbent molecules and Nb/G are shown in Fig. 1.

The adsorption energy (E_a), adsorption distance (d), the Hirshfeld charges (Q), work function (WF) of adsorbent molecule on the Nb/G surface are calculated, and electron localization function (ELF) is plotted for the orbital overlap of molecule Nb/G surface. The E_a is given by

$$E_a = E_{\mathrm{Nb/G+X}} - (E_{\mathrm{Nb/G}} + E_{\mathrm{X}}) \quad (1)$$

where, $E_{\mathrm{Nb/G+X}}$, $E_{\mathrm{Nb/G}}$ and E_{X} are the total energies of Nb/G with adsorbent molecules, isolated Nb/G surface and adsorbent molecules, respectively, and d is the equilibrium atom-to-atom nearest distance between adsorbent molecule and Nb/G.

III. Results and Discussion

In order to understand the interaction between the molecule and Nb/G surface, each molecular interface is discussed individually. Note that the optimized position and orientation of adsorbent molecule depend on the initial orientation of adsorbent molecules over Nb/G.

This article has been accepted for publication in a future issue of this journal, but has not been fully edited. Content may change prior to final publication. Citation information: DOI 10.1109/LED.2017.2787203, IEEE Electron Device Letters

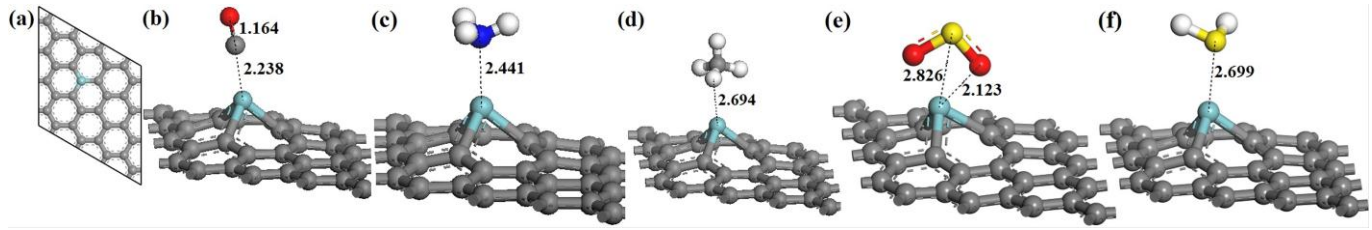

Fig. 1. Geometrically optimized and most favorable structure of Nb/G with (a) 4×4 graphene supercell with Nb doped, (b) CO, (c) NH_3, (d) CH_4, (e) SO_2, and (f) H_2S molecule. Dotted line and corresponding number in (Å) represents the distance between the atoms. The grey, cyan, red, white, dark blue, and yellow balls represent C, Nb, O, H, N, and S atoms, respectively.

CO adsorption: Adsorption of CO molecule on Nb/G is studied for three configurations of CO, viz. vertical orientation with O atom closer to Nb atom (VC1), vertical orientation with C atom closer to Nb atom (VC2) and the horizontal configuration (HC) of CO molecule symmetrically above the Nb/G surface. The nearest distance *d* is 2.37, 2.246 and 2.238 from the Nb atom and corresponding E_a are 0.32, -0.49 and -0.53 eV, respectively, for three configurations. HC has the lowest E_a and is most stable. Fig. 1(b) shows the HC and adsorption properties given in Table I. The *d* in VC2 and HC case is less than the sum of covalent radius (Nb=1.64 Å and C=0.69 Å) [19]. The total density of states (DOS) and atom projected density of states (PDOS) for Nb/G-CO are plotted in Fig. 2(a) and (b). A deviation in DOS is observed in between Fermi level and 2 eV, which occurs due to contribution from C *p* orbital of CO molecule with the Nb/G *p*, and Nb/G *d* orbitals. The overlapping of the C *p*, O *p* and Nb/G *p* orbitals is observed in the range -8 to -6 eV. The mixing of orbitals causes small charge transfer and redistribution over the interacting region. The population analysis for Hirshfeld charge transfer shows that -0.063 *e* charge is transferred from Nb/G surface to the CO molecule, suggesting that CO acts as an acceptor. Bond length after the adsorption is 1.164 Å, which is decreased from 1.171 Å of an isolated optimized CO molecule. ELF for Nb/G-CO is plotted in Fig. 3(a) and it shows presence of electron localization overlap in-between Nb/G and CO molecule. Combination of these parameters, i.e., *d* with covalent radii, E_a, deviation in DOS near Fermi energy and presence of electron localization overlap suggests that adsorption of CO on Nb/G is chemisorption.

NH_3 adsorption: Adsorption of NH_3 is studied for two configurations of NH_3, viz. vertical configuration with three H atoms near the Nb atom (VC1) and away from the Nb atom (VC2) above Nb/G surface. Here, the value *d* is 2.443, and 2.441 Å with E_a of -0.63 eV for both the configurations. Though the initial orientations of NH_3 molecule in the two configurations are opposite, they result into the identical structures after optimization. Fig. 1(c) shows the configuration VC2 with adsorption properties given in Table I. The *d* values for both the configurations are outside the sum of covalent radius (Nb=1.64 Å and N=0.71 Å), [19], but within the sum of Van der walls radius (Nb=2.15 Å and N=1.6 Å) [20]. The total DOS and PDOS for Nb/G-NH_3 are plotted in Fig. 2(c) and (d). There is small change in DOS at ~1 eV, which comes from the contribution of N *p* orbital overlap with Nb/G *p* and Nb/G *d* orbitals. Small difference in peak is observed near -7 eV also, which results due to the N *p* orbital overlap with Nb/G *p*. NH_3 has a lone pair of electrons available for interaction between nearby surface. The population analysis for Hirshfeld charge transfer shows that 0.236 *e* charge is transferred to Nb/G surface from the NH_3 molecule, suggesting that NH_3 acts as a donor. Bond length after the adsorption is 1.025 Å, slightly decreased from 1.031 Å and bond angle is 106.7° decreased from 107.8° of an isolated optimized NH_3 molecule. ELF for Nb/G-NH_3 is plotted in Fig. 3(b) and it shows presence of electron localization overlap in-between Nb/G and NH_3 molecules. Combination of all these properties, i.e., *d* with covalent radii and van der walls radius, high E_a, small deviation at ~1 eV and presence of electron localization overlap, suggests the physisorption nature of NH_3 over Nb/G surface.

TABLE I
COMPARISON OF ADSORPTION ENERGY (E_a), ADSORPTION DISTANCE (*d*), HIRSHFELD CHARGE TRANSFER (*Q*) OF THE GAS MOLECULE (X) ON Nb/G, N/G (NITROGEN DOPED GRAPHENE) AND G (GRAPHENE) SHEETS

SYSTEM	E_a (eV)	*d* (Å)	*Q* (*e*)	*References*
Nb/G-CO	-0.53	2.238	-0.063	THIS WORK
N/G–CO	-0.14	3.15	0	[24]
Nb/G-NH_3	-0.63	2.441	0.236	THIS WORK
N/G-NH_3	-0.12	2.86	0.04	[24]
Nb/G-CH_4	-0.12	2.694 (Nb -H) 2.844 (Nb -C)	0.093	THIS WORK
G-CH_4	-0.45	3.14 (C-C)	0.011	[6]
Nb/G-SO_2	-0.32	2.123	-0.293	THIS WORK
G-SO_2	-0.314	3.368	-0.067	[25]
Nb/G-H_2S	-1.68	2.699	0.167	THIS WORK
G-H_2S	-0.11	3.28	0	[26]

CH_4 adsorption: Adsorption of CH_4 is studied for two configuration of CH_4 viz. vertical orientation with three H atoms near Nb atom (VC1) and away from the Nb atom (VC2) above the Nb/G surface. *d* is 2.7 and 2.694 Å from the Nb atom and corresponding E_a are -0.11 and -0.12 eV, respectively for two configurations. Though the initial orientations of CH_4 molecule in the two configurations are opposite, they results into the identical structures after optimization. The lowest E_a configuration VC2 is shown in Fig. 1(d) and the adsorption properties given in Table I. All H atoms are at ~2.7 Å distance from Nb atom. *d* in each case are outside the sum of covalent radius (Nb=1.64 Å and H=0.31 Å), [17], but is below the sum of the Van der walls radius (Nb=2.15 Å and C=1.7 Å), [20]. The total DOS and PDOS for Nb/G-CH_4 are plotted in Fig. 2(e) and (f). There is no

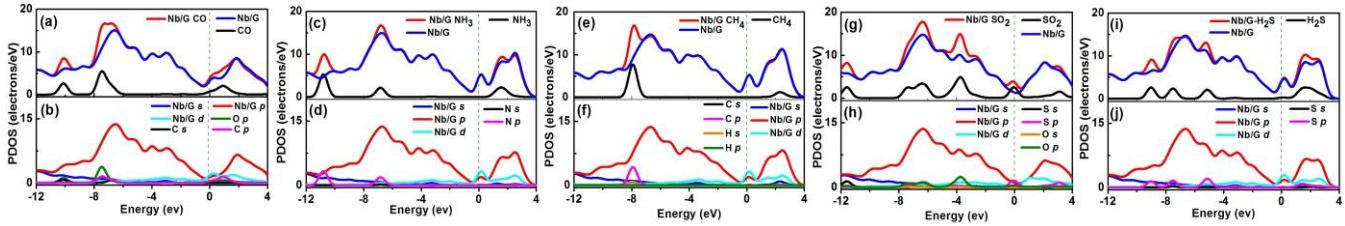

Fig. 2. Density of states comparison of Nb/G with adsorbent molecules over the surface. PDOS for specific orbital contribution in DOS (a) & (b) CO, (c) & (d) NH_3, (e) & (f) CH_4, (g) & (h) SO_2, and (i) & (j) H_2S molecules.

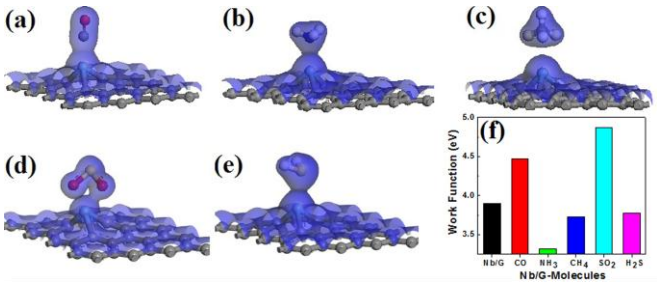

Fig. 3. Electron localization function (ELF) plot for (a) Nb/G-CO, (b) Nb/G-NH_3, (c) Nb/G-CH_4, (d) Nb/G-SO_2, (e) Nb/G-H_2S. (f) Comparison of work functions of Nb/G with the adsorbents.

deviation in DOS in -7 eV to 4 eV range, which suggests that CH_4 is weekly adsorbed on Nb/G. The charge of 0.093 *e* is induced to Nb/G surface from the CH_4 molecule, suggesting that CH_4 acts as a weak donor. Bond length after the adsorption is ~1.103 Å, almost unchanged from the isolated optimized CH_4. Electron localization plot as shown in Fig. 3(c) also suggests that no orbital overlap exists between the CH_4 and Nb/G surface. Thus, we conclude the weak physisorption of CH_4 over Nb/G surface.

SO_2 adsorption: Adsorption of SO_2 is studied for three configurations viz. vertical with S atom above the Nb atom and two O atom at the opposite side of Nb atom (VC1) and O at the near side of Nb atom (VC2), and horizontal configuration with S atom above the Nb atom (HC) over the Nb/G surface. The *d* values are 2.51, 2.123 and 2.148 Å from the Nb atom, and corresponding E_a are -0.026, -0.32 and -0.29 eV, respectively for the three configurations. VC2 has the lowest E_a and is most stable. Fig. 1(e) shows the VC2 with adsorption properties summarized in Table I. The *d* value in VC2 is lower the sum of covalent radius (Nb=1.64 Å and O=0.66 Å), [19]. Total DOS and PDOS of Nb/G-SO_2 are plotted in Fig. 2(g) and (h). Significant change is observed in DOS near Fermi level (-0.5 eV to 0.5 eV), which results from S *p* orbital hybridization with Nb/G *p* orbital. Deviation in DOS in -8 eV to -2 eV range results from O *p* orbital hybridization with Nb/G *p* orbital. The charge of 0.293 *e* is transferred from Nb/G surface to the SO_2 molecule, suggesting that the SO_2 acts as an acceptor. Bond length after the adsorption is ~1.59 Å, slightly increased from 1.543 Å of an isolated optimized SO_2 molecule. ELF for Nb/G-SO_2 is plotted in Fig. 3(d) and it shows presence of electron localization overlap in-between Nb/G and SO_2 molecule. By looking at these properties, we conclude that adsorption of SO_2 on Nb/G is chemisorption.

H_2S adsorption: Adsorption of H_2S is studied for three configurations, viz. vertical configuration with S atom above the Nb atom and two H atom at the opposite side of Nb atom (VC1) and at the same side of Nb atom (VC2), and horizontal configuration with sulphur atom above the Nb atom (HC) over the Nb/G surface. The *d* values are 2.699, 2.701 and 2.710 Å from the Nb atom, and the corresponding E_a are -1.68, -0.84 and -0.84 eV, respectively, for three configurations. VC1 configuration has the lowest E_a and is most stable. Fig. 1(f) shows the VC1 with adsorption properties given in Table I. The *d* value in each case is close to the sum of covalent radius (Nb=1.64 Å and S=1.05 Å), [19]. Total DOS and PDOS of Nb/G-H_2S are plotted in Fig. 2(i) and (j). Small deviation observed in DOS of Nb/G and Nb/G-H_2S near (1 to 3 eV) results from the overlapping of S *p* orbital with Nb/G *p* and Nb/G *d* orbitals. Deviation observed near -5 eV results from weak orbital overlap of S *p* with Nb/G *p* orbital. The charge of 0.167 *e* is transferred from H_2S to the Nb/G surface, suggesting the electron donor nature of H_2S. Bond length after the adsorption is 1.36 Å, slightly decreased from 1.39 Å of an isolated optimized H_2S molecule. ELF for Nb/G-H_2S is plotted in Fig. 3(e) and it shows the presence of electron localization overlap in-between Nb/G and H_2S molecule. Based on the above, we conclude that adsorption of SO_2 on Nb/G is physisorption.

Though experimental study on doped graphene for gas sensing application is rare, DFT studies on doped graphene suggest that doping improves the gas sensor performance [21], [22]. Experimental report on gas sensing performance of pristine graphene showed change in the conductivity with adsorbent revealing the donor/acceptor nature of adsorbents [2]. Comparison of Nb/G-X adsorption properties with other reported works are summarized in Table I. We found that CO and NH_3 has more affinity towards Nb/G as compared to that of pristine graphene (G) [6] and boron or nitrogen doped graphene [22], based on E_a, *d*, and *Q* values. Chen et al. [6] showed a higher E_a for CH_4 adsorption, though our calculation for pristine graphene shows consistently lower E_a (~0.18 eV) and negligible charge (-0.03 e) transfer as compared to those of Nb/G for CH_4. Similarly, SO_2 and H_2S have more affinity towards Nb/G, rather than pristine G.

Calculation of WF is important for exploring the possibilities of adjusting the electronic and optical properties, e.g., absorption spectrum, energy loss-function etc., for Nb/G through the adsorption of small molecules. WF is calculated from $\Phi = E_{vac} - E_F$, where E_{vac} and E_F are the energies of the vacuum level and of the Fermi level [23]. WF for Nb/G with and without adsorbents are plotted and shown in Fig. 3(f). Here, WF of Nb/G sheet is 3.89 eV, decreased from ~4.26 eV of an isolated graphene [23] as Nb is an electron rich 4*d* transition atom. Electron withdrawing adsorbent molecules (CO, and SO_2), over Nb/G surface will increase the work function of Nb/G-X system as there will be less localized electron in Nb/G surface. Quantity of charge transfer for SO_2 is greater than the CO molecule and thus we expect the WF to increase further for Nb/G-SO_2. Electron donating adsorbents (NH_3, H_2S, and CH_4) on the Nb/G surface will reduce the work function of Nb/G-X system as there will be more localized electrons in the Nb/G surface. Strongest electron donor NH_3 will have lowest WF. CH_4 and H_2S are weakly adsorbed with less charge induced over Nb/G surface; so, we expect small deviation from Fermi level of Nb/G surface. Electrodes and conductors with an appropriately tuned WF to facilitate efficient charge transport is an important aspect for optoelectronics and printed electronics applications where absorbents will change the performance of the material and hence presence of other molecules can be detected for specific determination of adsorbents. These results demonstrate the possibility of tuning the WF by the selective adsorption of molecules over Nb/G surface.

IV. Conclusion

We have presented the structural and electronic properties of Nb/G with adsorbents CO, NH_3, CH_4, SO_2, and H_2S molecules, using density functional theory method. The results of the adsorption energy, charge transfer, adsorption distance, and electron localization function show that the oxygen based molecules, viz. CO and SO_2, show chemisorption interaction with Nb/G and results in an increase of the work function. On the other hand, NH_3, CH_4, and H_2S molecules show physisorption when adsorbed on Nb/G. The adsorption of CH_4 and H_2S do small modification in WF, while for NH_3, it changes significantly. Comparison with pristine graphene for adsorption properties suggests Nb/G as superior material for gas sensing application. Our calculation predicts that Nb/G is highly sensitive to CO and SO_2 molecules, which may promote experimental efforts in this direction.

REFERENCES

[1] A. K. Geim and K. S. Novoselov, "The rise of graphene.," *Nat. Mater.*, vol. 6, pp. 183–191, 2007.

[2] F. Schedin, A. K. Geim, S. V. Morozov, E. W. Hill, P. Blake, M. I. Katsnelson, and K. S. Novoselov, "Detection of individual gas molecules adsorbed on graphene," *Nat. Mater.*, vol. 6, no. 9, pp. 652–655, 2007.

[3] M. H. Mohammed, F. N. Ajeel, and A. M. Khudhair, "Adsorption of gas molecules on graphene nanoflakes and its implication as a gas nanosensor by DFT investigations," *Chinese J. Phys.*, vol. 55, no. 4, pp. 1576–1582, 2017.

[4] M. Zhou, Y.-H. Lu, Y.-Q. Cai, C. Zhang, and Y.-P. Feng, "Adsorption of gas molecules on transition metal embedded graphene: a search for high-performance graphene-based catalysts and gas sensors," *Nanotechnology*, vol. 22, no. 38, p. 385502, 2011.

[5] X. Chen, L. Xu, L. L. Liu, L. S. Zhao, C. P. Chen, Y. Zhang, and X. C. Wang, "Adsorption of formaldehyde molecule on the pristine and transition metal doped graphene: First-principles study," *Appl. Surf. Sci.*, vol. 396, pp. 1020–1025, 2017.

[6] X. Chen, N. Yang, J. Ni, M. Cai, H. Ye, C. K. Y. Wong, S. Y. Y. Leung, T. Ren, and S. Member, "Density-Functional Calculation of Methane Adsorption on Graphenes," *IEEE Electron Device Lett.*, vol. 36, no. 12, pp. 1366–1368, 2015.

[7] M. D. Bhatt, G. Lee, and J. S. Lee, "Density Functional Theory (DFT) Calculations for Oxygen Reduction Reaction Mechanisms on Metal-, Nitrogen- co-doped Graphene (M-N2-G (M = Ti, Cu, Mo, Nb and Ru)) Electrocatalysts," *Electrochim. Acta*, vol. 228, pp. 619–627, 2017.

[8] X. Zhang, J. Guo, P. Guan, C. Liu, H. Huang, F. Xue, X. Dong, S. J. Pennycook, and M. F. Chisholm, "Catalytically active single-atom niobium in graphitic layers," *Nat. Commun.*, vol. 4, p. 1924, 2013.

[9] S. Y. Choi, Y. Kim, H. S. Chung, A. R. Kim, J. D. Kwon, J. Park, Y. L. Kim, S. H. Kwon, M. G. Hahm, and B. Cho, "Effect of Nb doping on chemical sensing performance of two-dimensional layered MoSe2," *ACS Appl. Mater. Interfaces*, vol. 9, no. 4, pp. 3817–3823, 2017.

[10] B. Delley, "From molecules to solids with the DMol3 approach," *J. Chem. Phys.*, vol. 113, no. 18, pp. 7756–7764, 2000.

[11] J. P. Perdew, K. Burke, and M. Ernzerhof, "Generalized Gradient Approximation Made Simple," *Phys. Rev. Lett.*, vol. 77, no. 18, pp. 3865–3868, 1996.

[12] M. Weinert and W. Davenport, "Fractional ocuupations and density-functional energies and forces," *Phys. Rev. B*, vol. 45, no. 23, pp. 709–712, 1992.

[13] R. S. Meng, M. Cai, J. K. Jiang, Q. H. Liang, X. Sun, Q. Yang, C. J. Tan, and X. P. Chen, "First Principles Investigation of Small Molecules Adsorption on Antimonene," *IEEE Electron Device Lett.*, vol. 38, no. 1, pp. 134–137, 2017.

[14] E. R. McNellis, J. Meyer, and K. Reuter, "Azobenzene at coinage metal surfaces: Role of dispersive van der Waals interactions," *Phys. Rev. B*, vol. 80, no. 20, pp. 1–10, 2009.

[15] H. C. Luo, R. S. Meng, H. Gao, X. Sun, J. Xiao, H. Y. Ye, G. Q. Zhang, and X. P. Chen, "First-principles Study of Nitric Oxide Sensor Based on Blue Phosphorus Monolayer," *IEEE Electron Device Lett.*, vol. 38, no. 8, pp. 1139–1142, 2017.

[16] X. P. Chen, L. M. Wang, X. Sun, R. S. Meng, J. Xiao, H. Y. Ye, and G. Q. Zhang, "Sulfur Dioxide and Nitrogen Dioxide Gas Sensor Based on Arsenene: A First-Principle Study," *IEEE Electron Device Lett.*, vol. 38, no. 5, pp. 661–664, 2017.

[17] B. Delley, "Hardness conserving semilocal pseudopotentials," *Phys. Rev. B*, vol. 66, no. 15, p. 155125, 2002.

[18] M. Pozzo, D. Alfè, P. Lacovig, P. Hofmann, S. Lizzit, and A. Baraldi, "Thermal expansion of supported and freestanding graphene: Lattice constant versus interatomic distance," *Phys. Rev. Lett.*, vol. 106, no. 13, pp. 135501-1-135501–4, 2011.

[19] B. Cordero, V. Gómez, A. E. Platero-Prats, M. Revés, J. Echeverría, E. Cremades, F. Barragán, and S. Alvarez, "Covalent radii revisited," *Dalt. Trans.*, no. 21, pp. 2832–2838, 2008.

[20] S. S. Batsanov, "Van der Waals Radii of Elements," *Inorg. Mater. Transl. from Neorg. Mater. Orig. Russ. Text*, vol. 37, no. 9, pp. 871–885, 2001.

[21] W. Yuan and G. Shi, "Graphene-based gas sensors," *J. Mater. Chem. A*, vol. 1, pp. 10078–10091, 2013.

[22] T. Wang, D. Huang, Z. Yang, S. Xu, and G. He, "A Review on Graphene-Based Gas/Vapor Sensors with Unique Properties and Potential Applications," *Nano-Micro Lett.*, vol. 8, no. 2, pp. 95–119, 2016.

[23] K. T. Chan, J. B. Neaton, and M. L. Cohen, "First-principles study of metal adatom adsorption on graphene," *Phys. Rev. B*, vol. 77, no. 23, pp. 1–12, 2008.

[24] Y. Zhang, Y. Chen, K. Zhou, and C. Liu, "Improving gas sensing properties of graphene by introducing dopants and defects : a first-principles study," *Nanotechnology*, vol. 20, p. 1885504, 2009.

[25] Q. Zhou, W. Ju, X. Su, Y. Yong, and X. Li, "Adsorption behavior of SO_2 on vacancy-defected graphene : A DFT study," *J. Phys. Chem. Solids*, vol. 109, pp. 40–45, 2017.

[26] Y. Zhang, L. Han, Y. Xiao, D. Jia, Z. Guo, and F. Li, "Understanding dopant and defect effect on H_2S sensing performances of graphene : A first-principles study," *Comput. Mater. Sci.*, vol. 69, pp. 222–228, 2013.